

Noble Gas Anions: A Theoretical Investigation of FNgBN⁻ (Ng = He–Xe)

Paola Antoniotti,[†] Stefano Borocci,[‡] Nicoletta Bronzolino,[‡] Patrizio Cecchi,[‡] and Felice Grandinetti^{*,*‡}

Dipartimento di Chimica Generale ed Organica Applicata, Università degli Studi di Torino, C.so M. D'Azeglio, 48, 10125 Torino, Italy, and Dipartimento di Scienze Ambientali, Università della Tuscia, L.go dell'Università, snc, 01100 Viterbo, Italy

Received: June 6, 2007; In Final Form: July 27, 2007

Noble gas anions of general formula FNgBN⁻ (Ng = He–Xe) have been investigated by MP2, coupled-cluster, and multireference-CI calculations with correlation-consistent basis sets. These species reside in deep wells on the singlet potential energy surface and are thermodynamically stable with respect to the loss of F, F⁻, BN, and BN⁻. They are unstable with respect to Ng + FBN⁻, but at least for Ng = Ar, Kr, and Xe, the involved energy barriers are high enough to suggest their conceivable existence as metastable species. The stability of FNgBN⁻ arises from the strong F⁻-stabilization of the elusive NgBN. The character of the boron–noble gas bond passes from purely ionic for FHeBN⁻ and FNeBN⁻ to covalent for FXeBN⁻.

1. Introduction

The noble gas elements, discovered in the 1890s by Ramsay and co-workers,¹ were for long time perceived as chemically inert. However, in 1962, Bartlett synthesized “Xe⁺PtF₆⁻”,² the first stable noble gas compound. Since then, numerous compounds containing krypton³ and xenon^{4,5} have been prepared in macroscopic amounts, and radon chemistry has been also explored by radiotracer techniques.⁶ Most recently, a covalent argon compound, HArF,⁷ and other krypton and xenon hydrides of general formula HNgX (Ng = Kr and Xe; X = electronegative atom or group) have been observed in cold matrices and characterized by infrared spectroscopy.⁸ Neutral compounds containing helium and neon are still missing, but their experimental search is encouraged, for example, by the theoretical prediction of metastable HHeF⁹ and of salts containing the FBeNg⁺ cations (Ng = He, Ne, Ar).¹⁰ Ions such as HeH⁺, He₂⁺, and HeNe⁺ were actually observed in the gas phase well before the Bartlett's experiment,¹¹ and various krypton and xenon cations have been also isolated in the solid state.^{3–5} The chemistry of the noble gas anions is instead less rich and variegated. The only bound species observed in the gas phase or isolated in the solid state are xenon anions such as XeF₃⁻,¹² XeF₅⁻,¹³ XeOF₅⁻,^{14,15} and XeO₆⁴⁻.¹⁶ All the other inert elements interact with anionic species such as H⁻,¹⁷ O⁻ and S⁻,^{18–20} the halogen anions,^{21–25} NO⁻,²⁶ HIH⁻,²⁷ HC₂⁻, and HC₄⁻²⁸ so to form at the most van der Waals complexes with predicted or computed binding energies of less than 1 or 2 kcal mol⁻¹. However, Hu and co-workers²⁹ have recently shown by ab initio calculations that the FNgO⁻ anions (Ng = He, Ar, Kr) are strongly bound species on the singlet surface, protected by sizable energy barriers from the largely exothermic dissociations into F⁻ + Ng + O(³P) and FO⁻ + Ng. From the general point of view, the remarkable stability of FNgO⁻ reflects a novel and somewhat unexpected structural motif in noble gas chemistry, namely the strong F⁻-stabilization of the singlet NgO, a species

only marginally stable for Ng = Ar³⁰ and Kr³¹ and completely unstable for Ng = He.³² We report here a computational investigation on the structure, stability, and properties of FNgBN⁻ (Ng = He–Xe), a novel group of anions whose stability arises from the F⁻-stabilization of the elusive NgBN complexes.^{33,34} These species are also isoelectronic with FNgBO,³⁵ one of the numerous neutral noble gas “insertion” compounds recently disclosed by theoretical calculations.^{34,36–41} A further investigation of inserted species of the general type XNgY⁻ could reveal novel stable or metastable anions of the noble gases.

2. Computational Details

The calculations were performed using Unix versions of the Gaussian03⁴² and MOLPRO 2000.1⁴³ sets of programs installed on a Alphaserver 1200 and a HP Proliant DL585 machine. The employed basis sets were the Dunning's correlation consistent double- and triple- ζ , augmented with diffuse functions (aug-cc-pVDZ and aug-cc-pVTZ).⁴⁴ For the Xe atom, the Stuttgart/Dresden (SDD) basis set with relativistic effective core potential⁴⁵ was employed, and the presently used basis sets will be therefore denoted as aug-cc-pVDZ/SDD and aug-cc-pVTZ/SDD. The geometry optimizations were performed at the second-order Møller–Plesset⁴⁶ (MP2) and at the coupled cluster level of theory^{47,48} (frozen-core approximation) including the contribution from single and double substitutions and an estimate of connected triples, CCSD(T). For the open-shell species, we used the spin-restricted coupled cluster theory as implemented in MOLPRO.^{49,50} The geometries of FHeBN⁻ and FNeBN⁻ were also optimized at the multireference-SCF level of theory, using a full-valence active space of 18 or 24 electrons distributed in 13 or 16 orbitals (CASSCF),⁵¹ respectively. The stationary points located at both the MP2 and CCSD(T) levels of theory were unambiguously characterized as energy minima or transition structures by computing their harmonic frequencies. The unscaled values were also used to calculate the zero-point vibrational energies (ZPE). The MP2/aug-cc-pVTZ/SDD atomic charges were calculated by natural bond orbital (NBO) analysis⁵² of the wave function and by the electrostatic potential-based

* To whom correspondence should be addressed. E-mail: fgrandi@unitus.it.

[†] Università degli Studi di Torino.

[‡] Università della Tuscia.

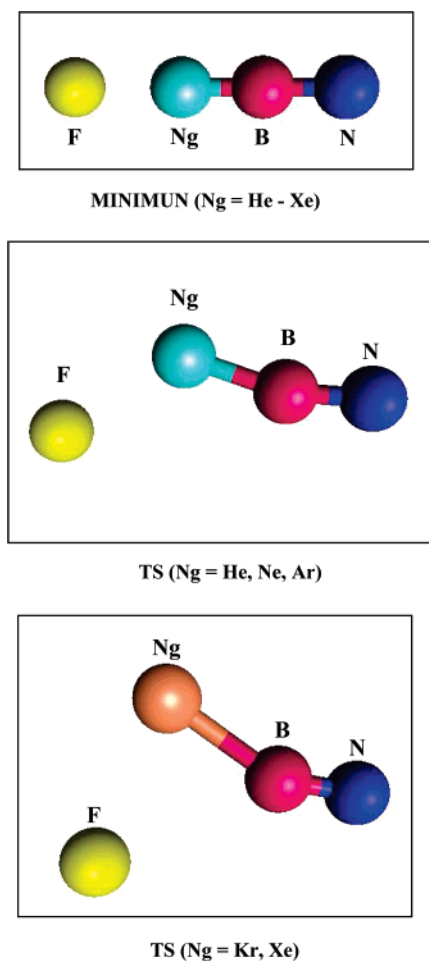


Figure 1. Connectivities of the FNgbN^- energy minima and transition structures.

methods ChelpG⁵³ and Merz–Kollman (MK) scheme.⁵⁴ The ChelpG calculations used the default value of point densities and Bondi's van der Waals radius of Kr (2.02 Å) and Xe (2.16 Å).⁵⁵ The MK electrostatic potential was fitted by a high point density (17 points/Å² and 10 layers around the van der Waals molecular surface) and using Bondi's van der Waals radius of Ar (1.88 Å), Kr, and Xe.⁵⁵ The chemical bonding analysis was based on the theory of atoms-in-molecules (AIM)⁵⁶ as implemented in the AIM2000 program package.⁵⁷ In particular, we calculated, at the MP2/aug-cc-pVTZ/SDD optimized geometries, the charge density ρ , the Laplacian of the charge density $\nabla^2\rho$, and the energy density H at the bond critical points (bcp), intended as the points on the attractor interaction lines where $\nabla\rho = 0$.

3. Results and Discussion

3.1. Structure of FNgbN^- (Ng = He–Xe). The presently investigated FNgbN^- anions are shown in Figure 1, and their geometrical parameters are listed in Table 1. The structures of KrBN, XeBN, and BN are also listed for comparison.

All the linear species were invariably characterized as true minima on the singlet MP2 and CCSD(T) potential energy surface. The bond distances are only less sensitive to the theoretical level and to the basis set, and we note larger differences of ca. 0.1 Å only in the B–Ne distance of FNeBN^- . Therefore, the MP2 and the CCSD(T) methods furnish a qualitatively and also quantitatively similar description of the structure of the FNgbN^- anions. This holds also true for their harmonic vibrational frequencies and energetics (with only few

minor exceptions; vide infra). It is however well-known from the literature^{58–62} that a correct description of the two most stable electronic states of BN ($X^3\Pi$ and $a^1\Sigma^+$) and of their subtle energy difference of less than 1 kcal mol⁻¹ requires multireference methods with large basis sets. Therefore, to appreciate whether the MP2 and the coupled cluster methods are indeed adequate to describe the FNgbN^- anions, we first computed their CCSD T1 diagnostics.⁶³ The values obtained for FArBN^- , FKrBN^- , and FXeBN^- resulted within the threshold of 0.02 usually accepted to support the validity of a monodeterminantal description of a reference wave function. The computed values of FHeBN^- , 0.022, and of FNeBN^- , 0.028, prompted us to repeat their geometry optimization at the CASSCF level of theory with the aug-cc-pVDZ basis set. The corresponding wave functions resulted dominated by the ground-state electronic configuration (C_0 larger than 0.95), and the computed bond distances (see Table 1) were in good agreement with the MP2 and the CCSD(T) estimates. This suggests that single-reference methods should give a qualitatively correct description of the electronic structure of the FNgbN^- anions.

From Table 1, the most relevant structural feature of the FNgbN^- anions is the quite short B–Ng distance, computed in particular at the CCSD(T)/aug-cc-pVTZ/SDD level of theory as 1.203, 1.573, 1.820, 1.961, and 2.153 Å, for Ng = He, Ne, Ar, Kr, and Xe, respectively. The corresponding F–Ng distances are instead considerably longer and increase from 1.725 to approximately 2.2–2.3 Å passing from FHeBN^- to the four heaviest congeners. In addition, the charge distribution analysis (vide infra) indicates that the F atom of any FNgbN^- carries a negative charge of nearly $-0.8/-0.9$ e. Therefore, from the structural point of view, the linear FNgbN^- must be viewed as ion–dipole complexes between F^- and NgBN. For KrBN and XeBN, such F^- –NgBN adducts are not surprising at all. The linear KrBN and XeBN are in fact energy minima on the CCSD(T)/aug-cc-pVTZ/SDD potential energy surface, stable at 0 K by 7.0 and 15.1 kcal mol⁻¹, respectively, with respect to dissociation into Kr or Xe and BN (for XeBN, this predicted stability is lower than a recent B3LYP/6-311++G(3df,3pd) estimate of ca. 28 kcal mol⁻¹³⁴). In addition, the optimized CCSD(T)/aug-cc-pVTZ/SDD bond distances of KrBN (B–Kr, 2.012 Å; B–N, 1.272 Å) and XeBN (B–Xe, 2.166 Å; B–N, 1.273 Å) are quite similar to the corresponding parameters of F^- –KrBN (B–Kr, 1.961 Å; B–N, 1.271 Å) and F^- –XeBN (B–Xe, 2.153 Å; B–N, 1.274 Å). The existence of F^- –HeBN, F^- –NeBN, and F^- –ArBN as energy minima is instead somewhat surprising and is probably the most relevant result from the present calculations. In fact, consistent with previous indications³³ from CASSCF and MP n calculations ($n = 2-4$), any attempt to optimize the geometry of HeBN, NeBN, and ArBN at the coupled cluster level of theory invariably resulted into dissociated He, Ne, Ar, and BN. Therefore, as already pointed out for the F^- –NgO anions (Ng = He, Ar, Kr),^{29a} at variance with “normal” ion–dipole complexes, the stability of F^- –HeBN, F^- –NeBN, and F^- –ArBN arises exclusively from the ability of the fluoride anion to fix on the singlet surface the intrinsically unstable HeBN, NeBN, and ArBN. The quantitative aspects of this stabilization and the ensuing bonding picture will be discussed in the forthcoming paragraphs. We simply note here that, at the CCSD(T)/aug-cc-pVTZ level of theory,^{29a} the F–He distance of F^- –HeO, 1.626 Å, and the F–Ar and F–Kr distances of F^- –ArO and F^- –KrO, both computed around 2.2 Å (F^- –NeO was not located as a minimum on the potential energy surface), are shorter than the corresponding F–Ng distances of F^- –HeBN, F^- –ArBN, and F^- –KrBN by only 0.1 Å. In addition, the F–Ng

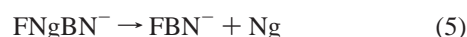
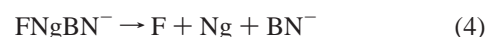
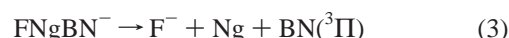
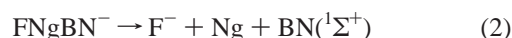
TABLE 1: Optimized Bond Lengths (Å) and Bond Angles (deg) of the FNgBN⁻ Energy Minima and Transition Structures (TS) (Figure 1)

species	method/basis set	min			TS				
		F–Ng	B–Ng	B–N	F–Ng	B–Ng	B–N	F–Ng–B	Ng–B–N
FHeBN ⁻	MP2/aug-cc-pVDZ	1.753	1.200	1.287	1.821	1.211	1.290	123.1	160.0
	MP2/aug-cc-pVTZ	1.733	1.196	1.277	1.800	1.202	1.279	124.4	160.0
	CCSD(T)/aug-cc-pVDZ	1.747	1.209	1.277	1.815	1.221	1.281	124.3	157.3
	CCSD(T)/aug-cc-pVTZ	1.725	1.203	1.266	1.791	1.208	1.269	125.5	158.9
	CASSCF/aug-cc-pVDZ	1.782	1.190	1.267					
FNeBN ⁻	MP2/aug-cc-pVDZ	2.268	1.638	1.303	2.299	1.665	1.306	129.9	165.4
	MP2/aug-cc-pVTZ	2.242	1.559	1.285	2.259	1.571	1.286	129.2	166.1
	CCSD(T)/aug-cc-pVDZ	2.266	1.668	1.288	2.302	1.700	1.292	135.4	161.9
	CCSD(T)/aug-cc-pVTZ	2.236	1.573	1.272					
	CASSCF/aug-cc-pVDZ	2.303	1.647	1.279					
FArBN ⁻	MP2/aug-cc-pVDZ	2.333	1.839	1.293	2.510	1.875	1.296	87.3	156.5
	MP2/aug-cc-pVTZ	2.291	1.808	1.281	2.470	1.838	1.284	86.6	156.9
	CCSD(T)/aug-cc-pVDZ	2.333	1.853	1.282	2.513	1.892	1.286	88.5	155.2
	CCSD(T)/aug-cc-pVTZ	2.293	1.820	1.270					
FKrBN ⁻	MP2/aug-cc-pVDZ	2.340	1.973	1.294	2.572	1.997	1.297	79.9	155.2
	MP2/aug-cc-pVTZ	2.301	1.946	1.283	2.521	1.965	1.285	79.2	155.9
	CCSD(T)/aug-cc-pVDZ	2.343	1.987	1.283	2.577	2.013	1.286	81.0	154.5
	CCSD(T)/aug-cc-pVTZ	2.311	1.961	1.271					
FXeBN ⁻	MP2/aug-cc-pVDZ/SDD	2.364	2.159	1.297	2.593	2.167	1.299	71.8	153.5
	MP2/aug-cc-pVTZ/SDD	2.349	2.139	1.285	2.567	2.142	1.287	71.3	154.5
	CCSD(T)/aug-cc-pVDZ/SDD	2.364	2.177	1.286	2.596	2.185	1.288	73.1	153.6
	CCSD(T)/aug-cc-pVTZ/SDD	2.349	2.153	1.274					
KrBN	MP2/aug-cc-pVDZ		2.030	1.301					
	MP2/aug-cc-pVTZ		1.984	1.287					
	CCSD(T)/aug-cc-pVDZ		2.072	1.286					
	CCSD(T)/aug-cc-pVTZ		2.012	1.272					
XeBN	MP2/aug-cc-pVDZ/SDD		2.170	1.301					
	MP2/aug-cc-pVTZ/SDD		2.141	1.288					
	CCSD(T)/aug-cc-pVDZ/SDD		2.204	1.286					
	CCSD(T)/aug-cc-pVTZ/SDD		2.166	1.273					
BN	MP2/aug-cc-pVDZ			1.335					
	MP2/aug-cc-pVTZ			1.326					
	CCSD(T)/aug-cc-pVDZ			1.285					
	CCSD(T)/aug-cc-pVTZ			1.275					

bond distances of the neutral FNgBO³⁵ and FNgBF₂^{41c} (Ng = Ar, Kr, Xe), recently investigated at the CCSD(T) and MP2 level of theory, respectively, with basis sets identical or comparable with those employed in the present study, are nearly independent of the noble gas and range around 2.1–2.2 Å. These values are also quite similar to the F–Ng distances of the well documented FNgH molecules, invariably computed as around 2.0–2.1 Å.⁶⁴ Combined with the results of the charge distribution analyses reported in these previous studies,^{35,41c,64} the anionic FNgO⁻ and FNgBN⁻ and the neutral FNgH, FNgBO, and FNgBF₂ share a common structural motif, namely the predominance of resonance formulas such as F⁻(NgO), F⁻(NgBN), F⁻(NgH⁺), F⁻(NgBO⁺), and F⁻(NgBF₂⁺). Therefore, their stability reflects at least partially the Coulomb interaction between F⁻ and a neutral or cationic moiety. In particular, for F⁻(NgO) and F⁻(NgBN), the high charge density of F⁻ polarizes the NgO and NgBN bonds and increases their bond energies. It is also of interest to compare other structural data of the FNgBN⁻ anions with those of FNgBO³⁵ and FNgBF₂^{41c}. At the CCSD(T)/aug-cc-pVTZ level of theory, the B–Ng distances of FNgBO, computed as 1.827 (Ng = Ar), 1.972 (Ng = Kr), and 2.173 Å (Ng = Xe) (FHeBO and FNeBO were not located as stable species), are nearly identical with the B–Ng distances of FArBN⁻, FKrBN⁻, and FXeBN⁻. For FNgBF₂, our computed MP2/aug-cc-pVTZ B–Ng distances of FArBN⁻, 1.808 Å, and FKrBN⁻, 1.946 Å, are only slightly shorter than the MP2/6-311++G(2d,2p) B–Ng distances of FAr–BF₂, 1.853 Å, and FKrBF₂, 1.994 Å. This suggests that the B–Ar and the B–Kr interaction is essentially independent of the B atom environment. On the other hand, at the MP2 level of theory with comparable basis sets (i.e., aug-cc-pVTZ/SDD

for FXeBN⁻ and FXeBO³⁵ and 6-311++G(2d,2p)/SDD for FXeBF₂^{41c}), the B–Xe distances are computed as 2.139, 2.155, and 2.435 Å, respectively, thus suggesting a more pronounced effect of the B atom environment on the boron–xenon interaction. Interestingly, at the B3LYP/6-311++G(3df,3pd) level of theory, the B–Xe distance of XeBN, HXeBNH, and HXeB₃N₅H₅ were computed as 2.160, 2.494, and 2.496 Å, respectively³⁴ (our CCSD(T)/aug-cc-pVTZ/SDD Xe–BN distance is 2.166 Å). The larger polarizability of xenon is probably responsible for these non-negligible effects of the chemical environment on the boron–xenon distance.

3.2. Dissociation Energies and Stabilities. The stability of the FNgBN⁻ anions on the singlet surface strictly depends on the energetics and the activation barriers of the following unimolecular dissociations:



The relevant MP2/aug-cc-pVTZ/SDD and CCSD(T)/aug-cc-pVTZ/SDD energy data are listed in Table 2.

For FKrBN⁻ and FXeBN⁻ the ΔE of reaction 1 is as large as 47 and 54 kcal mol⁻¹, respectively (as noted above, HeBN, NeBN, and ArBN are not stable on the singlet surface). For

TABLE 2: Dissociation Energies at 0 K (kcal mol⁻¹) of the FNgBN⁻ Anions (Reference Species) Calculated with the aug-cc-pVTZ/SDD Basis Set

species	method	F ⁻ + NgBN ^a	F ⁻ + Ng + BN(¹ Σ ⁺)	F ⁻ + Ng + BN(³ Π)	F + Ng + BN ⁻	Ng + FBN ⁻	barrier ^b
FHeBN ⁻	MP2		27.3	36.3	57.4	-116.7	1.6
	CCSD(T)		26.6	26.8	32.7	-116.7	1.4 ^c /1.5 ^d
FNeBN ⁻	MP2		12.0	21.0	42.2	-131.9	0.6
	CCSD(T)		11.4	11.6	17.5	-131.9	0.5 ^c
FArBN ⁻	MP2		42.6	51.6	72.7	-101.4	12.9
	CCSD(T)		40.7	40.9	46.7	-102.7	12.4 ^c
FKrBN ⁻	MP2	47.4	56.6	65.6	86.8	-87.3	18.9
	CCSD(T)	47.4	54.4	54.6	60.5	-88.9	18.6 ^c
FXeBN ⁻	MP2	53.6	71.1	80.1	101.2	-72.9	24.8
	CCSD(T)	54.0	69.0	69.2	75.1	-74.3	24.6 ^c

^a HeBN, NeBN, and ArBN are not energy minima. ^b Energy barrier for the reaction FNgBN⁻ → Ng + FBN⁻. ^c Calculated at the CCSD(T)/aug-cc-pVDZ optimized geometry. ^d Calculated at the CCSD(T)/aug-cc-pVTZ optimized geometry.

comparison, at the CCSD(T)/aug-cc-pVTZ level of theory, the dissociation of FKrO⁻ into F⁻ and KrO results endothermic by 37.4 kcal mol⁻¹,^{29a} although the F–KrO⁻ bond distance, 2.259 Å, is slightly shorter than F–KrBN⁻, 2.311 Å. This probably arises from the dipole moment of KrBN larger than KrO (9.1 vs 2.7 D at the CCSD(T)/aug-cc-pVTZ level of theory). For all the FNgBN⁻'s, reaction 2 is also appreciably endothermic. In particular, for FHeBN⁻, FNeBN⁻, and FArBN⁻, the computed ΔE's provide an overall quantitative estimate of the ability of the fluoride anion to fix the intrinsically unstable HeBN, NeBN, and ArBN. Interestingly, the F⁻-induced stabilization of ArBN, computed as 40.7 kcal mol⁻¹ at the CCSD(T)/aug-cc-pVTZ level of theory, is higher than HeBN, 26.6 kcal mol⁻¹, but the stabilization of NeBN is lower than that of HeBN by nearly 15 kcal mol⁻¹. This somewhat unexpected trend closely resembles the predicted relative stability of other complexes of the lightest noble gases. In particular, Frenking and co-workers noted so far³³ that once corrected for the basis set superposition error (BSSE), the MP4(SDTQ)/6-311G(2df,2pd) stabilities of the OBeNg adducts (Ng = He–Ar) increased in the unexpected order OBeNe < OBeHe < OBeAr. Similarly, we have subsequently found⁶⁵ that the BSSE-corrected CCSD(T)/6-311G(d,p) and CCSD(T)/6-311++G(2df,2p) dissociation energy of HNBeNe is lower than that of HNBeHe by ca. 1.5 kcal/mol. As noted previously,³³ these anomalous trends could reflect the at least partial inadequacy of the counterpoise method to correct for the BSSE, and it was not possible to get a safe conclusion of which of XBeHe and XBeNe (X = O or NH) is actually more stable. In any case, our results on the F⁻-induced stabilization of NgBN provide further evidence for an intrinsically difficult stabilization of neon. Interestingly, we remark here that HNeF is the only neutral HNgF which was not located as an energy minimum at the coupled cluster level of theory.¹⁰

The energy changes of reaction 3 simply differ from those of reaction 2 by the singlet–triplet gap of BN. At the CCSD(T)/aug-cc-pVTZ level of theory, the singlet state is more stable than the triplet by 0.2 kcal mol⁻¹ (the overestimated MP2 difference is 9 kcal mol⁻¹), while the experiments point to a triplet state which is more stable than the singlet by nearly 0.5 kcal mol⁻¹.^{66,67} At this stage of experience, however, this result is not surprising. It is in fact well-known^{59–62} that coupled cluster methods, even in conjunction with large basis sets, fail to predict the correct order and energy difference between the two most stable electronic states of BN. In any case, this does not alter the conclusion that any FNgBN⁻ is thermodynamically stable with respect to dissociation into F⁻, Ng, and singlet or triplet BN. The dissociation into F, Ng, and BN⁻ is even more endothermic, as the electron affinity of BN, 3.160 ± 0.005 eV,⁶⁷ is lower than that of the F atom, 3.4 eV.⁶⁸ From Table 2, at the CCSD(T)/aug-cc-pVTZ level of theory, this difference nicely

reflects in the ΔE's of reaction 4, predicted to be higher than reaction 3 by 5.9 kcal mol⁻¹ (0.26 eV). Therefore, all the FNgBN⁻ anions are predicted to be by far stable with respect to any dissociation (1)–(4). We note also that the MP2 method overestimates the dissociation energies of reactions 3 and 4 by ca. 10 and 25 kcal mol⁻¹, respectively. These results are in line with a recent study by Hu and co-workers⁶⁹ who found that while the MP2 method was quite successful for studying the decomposition of XNgY into Ng and XY, it systematically overestimated the energies of the dissociation into X + Ng + Y. The overestimated MP2 ΔE of reaction 4 may also at least partially reflect the strong spin-contamination we have found for the UHF wave function of the doublet BN⁻. For any Ng, the unimolecular dissociation (5) is largely exothermic. The MP2 and CCSD(T) computed ΔE's are quite similar and range from ca. -130 kcal mol⁻¹ for FNeBN⁻ to ca. -75 kcal mol⁻¹ for FXeBN⁻. Therefore, any assessment of the kinetic stability of the singlet FNgBN⁻ requires a detailed evaluation of the activation barrier of reaction 5. We have thus ascertained that this process occurs through the bent transition structures shown in Figure 1. Their geometries were optimized at the MP2 level of theory with both the aug-cc-pVDZ and the aug-cc-pVTZ basis sets and at the CCSD(T)/aug-cc-pVDZ level of theory. For FHeBN⁻, the TS was also located at the CCSD(T)/aug-cc-pVTZ level of theory. However, similar to the energy minima, the obtained geometries (see Table 1) revealed as only less sensitive to the theoretical level and to the basis set. In addition, for any TS, the CCSD/aug-cc-pVDZ T1 diagnostic resulted within the threshold of 0.02. Passing from the minimum to the TS, we note the elongation of the Ng–F bond by ca. 0.1–0.2 Å, the closing of the Ng–B–N bond angle by ca. 25–30°, and the even more pronounced closing of the B–Ng–F bond angle, which reduces up to ca. 70–80° for F–Kr–BN⁻ and F–Xe–BN⁻. The imaginary frequencies are invariably associated with the F–Ng–B bending motion and are computed in particular at the CCSD(T)/aug-cc-pVDZ/SDD level of theory as 259.8i (Ng = He), 70.1i (Ng = Ne), 124.6i (Ng = Ar), 123.3i (Ng = Kr), and 121.2i (Ng = Xe) (the MP2/aug-cc-pVDZ/SDD and MP2/aug-cc-pVTZ/SDD values are quite similar). The activation barriers of reaction 5 are listed in Table 2. The MP2 and the CCSD(T) predicted values are nearly identical and amount to ca. 1.5, 0.5, 13, 19, and 25 kcal mol⁻¹, respectively, for Ng = He, Ne, Ar, Kr, and Xe. Quantitative criteria have been recently proposed for the metastability of the noble gas molecules XNgY (X and Y other than H).⁶⁹ In particular, to have a half-life of ca. 100 s in the gas phase at 100, 200, and 300 K, the dissociation into X + Ng + Y must have a barrier of 9, 17, and 25 kcal mol⁻¹, respectively, and the dissociation into Ng + XY must have barriers of 6, 13, and 21 kcal mol⁻¹, respectively. Therefore, while FArBN⁻ is predicted to be

TABLE 3: MP2/aug-cc-pVTZ/SDD Atomic Charges q (e) of the FNgBN⁻ Energy Minima and Transition Structures (Figure 1)

species	method	min				TS			
		F	Ng	B	N	F	Ng	B	N
FHeBN ⁻	NBO	-0.95	0.30	0.52	-0.88	-0.95	0.28	0.57	-0.90
	ChelpG	-0.93	0.44	0.27	-0.78	-0.89	0.31	0.43	-0.85
	MK ^a	-0.92	0.48	0.17	-0.73	-0.88	0.34	0.35	-0.81
FNeBN ⁻	NBO	-0.99	0.23	0.69	-0.93	-0.99	0.21	0.71	-0.94
	ChelpG	-0.97	0.39	0.31	-0.73	-0.94	0.31	0.41	-0.78
	MK ^a	-0.97	0.44	0.22	-0.69	-0.94	0.33	0.35	-0.75
FArBN ⁻	NBO	-0.95	0.50	0.33	-0.89	-0.98	0.41	0.47	-0.91
	ChelpG	-0.87	0.46	0.21	-0.80	-0.87	0.30	0.43	-0.86
	MK ^a	-0.87	0.50	0.12	-0.75	-0.86	0.33	0.35	-0.82
FKrBN ⁻	NBO	-0.92	0.60	0.21	-0.89	-0.97	0.48	0.39	-0.90
	ChelpG	-0.81	0.46	0.16	-0.81	-0.84	0.28	0.44	-0.88
	MK ^a	-0.81	0.46	0.17	-0.82	-0.83	0.31	0.35	-0.83
FXeBN ⁻	NBO	-0.90	0.73	0.06	-0.89	-0.95	0.57	0.28	-0.91
	ChelpG	-0.73	0.43	0.13	-0.83	-0.78	0.24	0.45	-0.91
	MK ^a	-0.73	0.47	0.04	-0.78	-0.76	0.26	0.34	-0.84
KrBN	NBO		0.47	0.26	-0.73				
	ChelpG		0.43	0.18	-0.61				
	MK ^a		0.48	0.08	-0.56				
XeBN	NBO		0.59	0.12	-0.71				
	ChelpG		0.46	0.16	-0.62				
	MK ^a		0.50	0.06	-0.56				
BN	NBO			0.64	-0.64				
	ChelpG			0.29	-0.29				
	MK ^a			0.26	-0.26				

^a The default number of points/Å² and number of layers were modified by IOp(6/41 = 10,6/42 = 17) in the route section of the Gaussian input file.

metastable on the singlet surface up to ca. 200 K, FKrBN⁻ and, especially, FXeBN⁻ are predicted to be metastable up to ca. 300 K. On the other hand, for FHeBN⁻ and FNeBN⁻, the activation barrier of reaction 5 is too small to support their conceivable existence as metastable species in the gas phase. The diatomic BN may be actually produced by laser vaporization,⁶⁶ and experiments could be probably attempted to obtain FNgBN⁻ (Ng = Ar, Kr, Xe), for example, in solid matrices. These conclusions closely resemble the predicted dynamical stability³⁵ of FArBO, FKrBO, and FXeBO and the negligible or even nonexistent barriers to the dissociation of FHeBO and FNeBO by the F–Ng–B bending motion. Compared with the isoelectronic FNgBO, the FNgBN⁻ anions (Ng = Ar, Kr, Xe) are thermodynamically more stable. At the CCSD(T)/aug-cc-pVTZ/SDD level of theory, the ΔE of reaction 4 is in fact higher than the dissociation energy into F + Ng + BO³⁵ by ca. 32 kcal mol⁻¹ for Ng = Ar, ca. 35 kcal mol⁻¹ for Ng = Kr, and ca. 25 kcal mol⁻¹ for Ng = Xe. Since the B–F bond of FBN⁻ is weaker than that of FBO (149.4 vs 159.6 kcal mol⁻¹), the dissociation of FNgBN⁻ into Ng and FBN⁻ is less exothermic than FNgBO by 30–50 kcal mol⁻¹. We note also that any FNgBF₂ (Ng = Ar, Kr, Xe),^{41c} HXeBNH, and HXeB₃N₃H₅³⁴ resulted kinetically stable on the singlet surface.

3.3. Charge Distribution and Bonding Analysis. The charge distribution and the AIM analysis of FNgBN⁻, KrBN, XeBN, and BN, reported in Tables 3 and 4 and in Figure 2, first confirm the structural assignment of the FNgBN⁻ anions as F⁻–NgBN ion–dipole complexes.

The negative charges of the F atoms range in fact around -0.8/-0.90 e, with a largest value of nearly -1 e for FNeBN⁻. In addition, at the bond critical point (bcp) of any F–Ng bond, the charge density is low, the corresponding Laplacian is positive, and the energy density, although decreasing from 0.040 (Ng = He) to -0.061 (Ng = Xe) hartree Å⁻³, is essentially vanishingly small. Overall, this suggests an ionic fluorine–noble gas interaction. Consistently, the Laplacian contour lines around the F atoms are essentially spheric, with only slight progressively increasing deformations from FHeBN⁻ to FXeBN⁻.

As to the nature of the boron–noble gas interaction, the bond between noble gases and closed-shell compounds, whether ionic or covalent or both, raises in general animated debate in the literature. If we turn to a recent exemplary case, the Au⁺–Ng complexes were theoretically predicted to be mainly covalent-like.⁷⁰ However, subsequent arguments based on higher order multipoles to describe induced polarization effects⁷¹ significantly reduced the amount of covalent interaction and supported the conclusion that “the need to invoke covalency within the Au⁺–Ng bond appears to be unproven, even for diffuse species such as Xe”.⁷¹ In addition, for elements as heavy as xenon, the use of the effective core potential and the consequent absence of an explicit representation of the core electron density makes the corresponding topological analysis problematical.⁷² In any case, the data of Tables 3 and 4 and Figure 2 support the following considerations. First, the computed total charges indicate that, in any FNgBN⁻, the nitrogen atom draws some electron density from both the boron and the noble gas atom, and this is enhanced by the presence of the fluoride anion. From Figure 2, this arises from the charge-depletion region, absent in the diatomic BN, around the B atom of FNgBN⁻. For FKrBN⁻ and FXeBN⁻, this “ σ hole” appears an intrinsic feature of the KrBN and XeBN complexes, and the presence of F⁻ simply enhances the charge transfer from Kr or Xe to BN (see Table 3). On the other hand, HeBN, NeBN, and ArBN are intrinsically unstable, and the origin of the σ hole around the B atoms of the corresponding FNgBN⁻ is therefore less clear. We therefore computed the contour lines diagram of the $-\nabla^2\rho(\mathbf{r})$ of a hypothetical F⁻–BN anionic complex with a B–F distance of 2.93 Å and a B–N distance of 1.28 Å and found that the B–N moiety is an essentially unperturbed diatomic BN. Therefore, the charge-depletion region around the B atom of FHeBN⁻, FNeBN⁻, and FArBN⁻ arises from the joint presence of the noble gas and the fluoride anion.

As to the nature of the boron–noble gas interaction, the available data clearly indicate a strong variability going in particular from FNeBN⁻ to FXeBN⁻. In the former species, the contour lines of the Laplace distribution around the Ne atom

TABLE 4: MP2/aug-cc-pVTZ/SDD AIM Analysis of the FNgBN⁻ Energy Minima (C_{∞v}) and Transition Structures (C_s) (Figure 1)^a

species	property	min			TS		
		F–Ng	B–Ng	B–N	F–Ng	B–Ng	B–N
FHeBN ⁻	ρ	0.369	0.803	1.722	0.309	0.736	1.719
	$\nabla^2\rho$	7.73	24.50	36.01	6.84	25.13	35.45
	H	0.040	-0.277	-1.656	0.046	-0.181	-1.659
FNeBN ⁻	ρ	0.173	0.475	1.594	0.170	0.447	1.592
	$\nabla^2\rho$	4.27	15.92	38.72	4.13	15.08	38.09
	H	0.058	-0.097	-1.409	0.055	-0.085	-1.411
FArBN ⁻	ρ	0.304	0.710	1.714	0.208	0.579	1.682
	$\nabla^2\rho$	5.12	7.10	34.29	3.72	9.07	35.16
	H	0.012	-0.547	-1.662	0.023	-0.364	-1.597
FKrBN ⁻	ρ	0.358	0.731	1.730	0.228	0.594	1.688
	$\nabla^2\rho$	5.18	1.78	32.92	3.62	5.49	34.55
	H	-0.012	-0.646	-1.702	0.014	-0.446	-1.614
FXeBN ⁻	ρ	0.388	0.724	1.738	0.258	0.600	1.689
	$\nabla^2\rho$	4.24	-3.74	31.53	3.44	1.24	33.64
	H	-0.061	-0.651	-1.731	-0.004	-0.509	-1.623
KrBN	ρ		0.544	1.631			
	$\nabla^2\rho$		6.48	36.86			
	H		-0.382	-1.491			
XeBN	ρ		0.574	1.649			
	$\nabla^2\rho$		2.59	35.57			
	H		-0.469	-1.535			
BN	ρ			1.115			
	$\nabla^2\rho$			41.83			
	H			-0.538			

^a The charge density ρ (e Å⁻³), the Laplacian of the charge density $\nabla^2\rho$ (e Å⁻⁵), and the energy density H (hartree Å⁻³) are calculated at the bond critical point on the specified bond.

TABLE 5: Harmonic Vibrational Frequencies (cm⁻¹) of the Linear FNgBN⁻ ^a

species	method/basis set	assignment				
		ν (F–Ng)	ν (B–Ng)	ν (B–N)	δ (F–Ng–B) ^b	δ (Ng–B–N) ^b
FHeBN ⁻	MP2/aug-cc-pVDZ	300 (80.9 ^c /76.2 ^d)	1217 (435.5 ^c /51.7 ^d)	1873 (1791.4 ^c /21.8 ^d)	146 (9.7 ^c /55.3 ^d)	326 (33.3 ^c /28.0 ^d)
	MP2/aug-cc-pVTZ	305 (82.8 ^c /76.6 ^d)	1248 (460.3 ^c /59.0 ^d)	1899 (1832.8 ^c /24.9 ^d)	142 (8.8 ^c /59.0 ^d)	316 (33.3 ^c /21.9 ^d)
	CCSD(T)/aug-cc-pVDZ	302 (82.0 ^c)	1222 (417.7 ^c)	1921 (2067.9 ^c)	137 (9.4 ^c)	286 (24.1 ^c)
	CCSD(T)/aug-cc-pVTZ	308 (80.5 ^c)	1262 (447.3 ^c)	1955 (2124.8 ^c)	138 (8.9 ^c)	283 (24.6 ^c)
FNeBN ⁻	MP2/aug-cc-pVDZ	190 (34.1 ^c /88.8 ^d)	429 (190.1 ^c /9.5 ^d)	1628 (1872.7 ^c /0.1 ^d)	52 (2.9 ^c /46.0 ^d)	177 (21.8 ^c /0.8 ^d)
	MP2/aug-cc-pVTZ	216 (44.9 ^c /74.8 ^d)	489 (243.4 ^c /8.5 ^d)	1699 (2038.5 ^c /0.9 ^d)	53 (3.1 ^c /49.6 ^d)	196 (26.7 ^c /1.1 ^d)
	CCSD(T)/aug-cc-pVDZ	177 (29.0 ^c)	397 (165.9 ^c)	1735 (2136.2 ^c)	47 (2.4 ^c)	123 (10.5 ^c)
	CCSD(T)/aug-cc-pVTZ	214 (43.6 ^c)	470 (226.4 ^c)	1801 (2300.3 ^c)	56.2 (3.4 ^c)	159 (17.7 ^c)
FArBN ⁻	MP2/aug-cc-pVDZ	261 (71.8 ^c /121.8 ^d)	465 (242.2 ^c /13.1 ^d)	1713 (2069.7 ^c /0.3 ^d)	89 (10.0 ^c /53.2 ^d)	254 (46.7 ^c /0.6 ^d)
	MP2/aug-cc-pVTZ	269 (77.2 ^c /127.9 ^d)	491 (266.0 ^c /16.6 ^d)	1748 (2154.7 ^c /0.5 ^d)	93 (10.9 ^c /53.2 ^d)	268 (52.0 ^c /0.3 ^d)
	CCSD(T)/aug-cc-pVDZ	263 (71.8 ^c)	453 (231.8 ^c)	1794 (2277.2 ^c)	88 (9.7 ^c)	239 (41.5 ^c)
	CCSD(T)/aug-cc-pVTZ	272 (78.0 ^c)	482 (257.6 ^c)	1833 (2374.6 ^c)	94 (11.0 ^c)	258 (48.3 ^c)
FKrBN ⁻	MP2/aug-cc-pVDZ	273 (84.9 ^c /172.1 ^d)	407 (162.0 ^c /24.0 ^d)	1706 (2052.6 ^c /0.3 ^d)	87 (9.5 ^c /50.8 ^d)	260 (48.0 ^c /0.8 ^d)
	MP2/aug-cc-pVTZ	287 (94.2 ^c /175.5 ^d)	425 (175.7 ^c /27.7 ^d)	1739 (2134.4 ^c /0.2 ^d)	90 (10.2 ^c /50.1 ^d)	270 (51.9 ^c /0.4 ^d)
	CCSD(T)/aug-cc-pVDZ	274 (84.5 ^c)	397 (154.8 ^c)	1789 (2263.3 ^c)	86 (9.2 ^c)	249 (44.2 ^c)
	CCSD(T)/aug-cc-pVTZ	284 (91.9 ^c)	414 (167.7 ^c)	1825 (2355.2 ^c)	90 (10.1 ^c)	262 (48.9 ^c)
FXeBN ⁻	MP2/aug-cc-pVDZ/SDD	298 (103.8 ^c /213.3 ^d)	379 (129.0 ^c /39.7 ^d)	1689 (2013.3 ^c /3.2 ^d)	86 (8.8 ^c /44.9 ^d)	255 (46.0 ^c /1.6 ^d)
	MP2/aug-cc-pVTZ/SDD	302 (107.0 ^c /213.6 ^d)	387 (133.7 ^c /39.8 ^d)	1722 (2092.0 ^c /3.0 ^d)	89 (9.4 ^c /45.5 ^d)	267 (50.0 ^c /1.1 ^d)
	CCSD(T)/aug-cc-pVDZ/SDD	298 (102.4 ^c)	369 (123.2 ^c)	1733 (2224.4 ^c)	85 (8.6 ^c)	249 (43.7 ^c)
	CCSD(T)/aug-cc-pVTZ/SDD	302 (106.3 ^c)	379 (129.0 ^c)	1809 (2316.0 ^c)	89 (9.4 ^c)	264 (49.1 ^c)

^a Force constants (N m⁻¹) and IR intensities (km mol⁻¹) are given in parentheses. ^b Doubly degenerate bending motion. ^c Force constant. ^d IR intensity.

are nearly spheric, and at the bcp on the B–Ne bond, the Laplacian of the charge density is positive and the energy density is vanishingly small. This suggests an ionic boron–neon interaction. The bonding picture of FXeBN⁻ is instead clearly opposite. At the bcp on the B–Xe bond, the Laplacian of the charge density and the energy density are both negative, as usually occurs for covalent interactions.⁷³ Consistently, the contour lines of the Laplace distribution show a uniform region of charge concentration around the boron–xenon bond. As for FHeBN⁻, FArBN⁻, and FKrBN⁻, the contour lines of the Laplace distributions around the noble gas show increasing deformations in the order He < Ar < Kr. In addition, at the bcp on the corresponding B–Ng bonds, the Laplacian of the

charge density and the energy density regularly decrease and, in particular, H reaches a negative value of -0.651 hartree Å⁻³ for FKrBN⁻. This suggests that the boron–noble gas interaction, essentially ionic in FHeBN⁻ and FArBN⁻, has an onset of covalent bond in FKrBN⁻.

From Tables 3 and 4, in the passage from any FNgBN⁻ energy minimum to the corresponding transition structure, the charge distribution and the topology of the charge density show appreciable but still minor changes. This indicates that the dissociation (5) occurs by the movement of a fluoride anion which “walks around” the NgBN moiety.

3.4. Harmonic Vibrational Frequencies. The harmonic vibrational frequencies, force constants, and IR intensities of

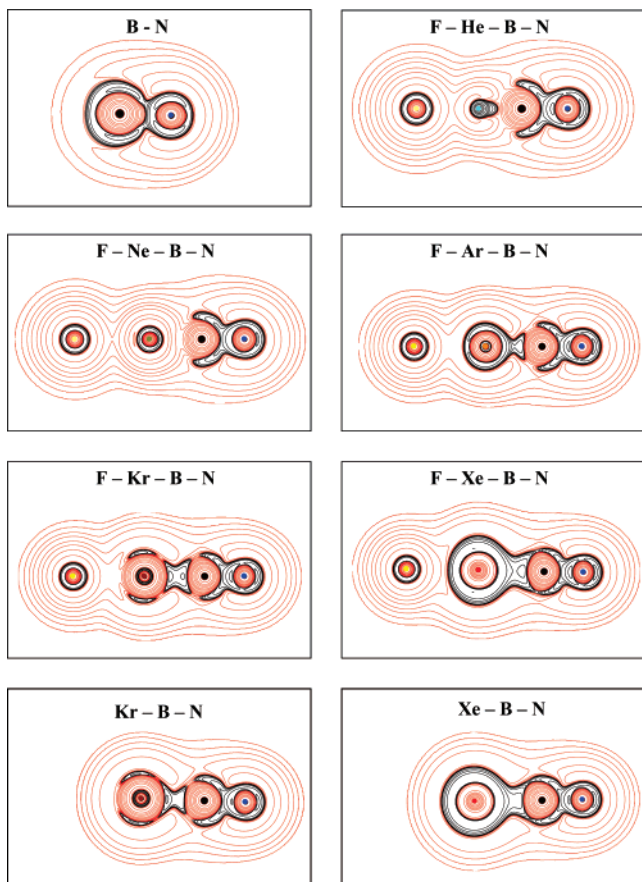


Figure 2. Contour line diagrams of the MP2/aug-cc-pVTZ/SDD Laplacian of the electronic charge density $-\nabla^2\rho(\mathbf{r})$ of BN, KrBN, XeBN, and FNgBN⁻. Red and black lines are in regions of charge depletion ($-\nabla^2\rho(\mathbf{r}) < 0$) and charge concentration ($-\nabla^2\rho(\mathbf{r}) > 0$), respectively.

the FNgBN⁻ anions are listed in Table 5. These values are only less sensitive to the theoretical level and to the basis set, and we will refer in particular to the CCSD(T)/aug-cc-pVTZ/SDD estimates.

The nuclear motions are in general only weakly coupled, and one easily recognizes the five expected molecular vibrations, namely three stretching and two doubly degenerate bending motions. For any vibrational mode, the wavenumber of FHeBN⁻ is the highest among the various FNgBN⁻. This trend reflects however the combined effect of force constants, which are not invariably the highest, and lowest reduced mass. The only exception is the B–He stretching frequency, whose highest value of 1262 cm⁻¹ parallels a highest force constant of 447 N m⁻¹. If we pass to the heaviest congeners, the B–Ng stretching frequencies (and the corresponding force constants) significantly reduce and follow a decreasing periodic trend from 482 to 379 cm⁻¹ passing from FArBN⁻ to FXeBN⁻. The IR intensities of these motions are also relatively high, and their observation could be structurally diagnostic for in case produced FNgBN⁻ anions. For FNeBN⁻, the B–Ne stretching frequency of 470 cm⁻¹ is lower than that for FArBN⁻, and the wavenumbers of all the other vibrational motions are the lowest among the various FNgBN⁻ anions. This parallels the lowest predicted thermodynamic and kinetic stability of the neon-containing anion. The B–N stretching frequency, predicted at 1955 cm⁻¹ for FHeBN⁻ and around 1800 cm⁻¹ for the four heaviest congeners, is invariably higher than the harmonic frequency of the singlet BN, computed as 1717 cm⁻¹ at the CCSD(T)/aug-cc-pVTZ level of theory and experimentally measured as 1712

cm⁻¹.⁷⁴ Therefore, the in case formation of FNgBN⁻ from BN is expected to be accompanied by an appreciable blue-shift of this motion. However, with the only exception of FHeBN⁻, the IR intensity of any B–N stretching is predicted as rather weak. Finally, all the F–Ng stretching frequencies have strong IR intensities, but they fail in the rather inconvenient far-infrared region. The computed wavenumbers of nearly 300 cm⁻¹ are quite similar, for any noble gas, to those predicted for the FNgO⁻ anions.^{29a}

4. Concluding Remarks

Searching for novel noble gas anions still remains a fascinating experimental and theoretical challenge. The simple fixation of the inert elements by X⁻ usually results in very weak NgX⁻ van der Waals complexes. The recent work by Hu and co-workers²⁹ and the present calculations disclose however an alternative strategy, which consists of the fixation of the noble gases into anionic species such as FNgO⁻ and FNgBN⁻. The stability of these ions arises from the strong F⁻ stabilization on the singlet surface of intrinsically unstable or only marginally stable complexes such as the diatomic NgO and the triatomic NgBN. At this stage of experience, it is of interest to speculate whether anionic species other than F⁻ could stabilize not only NgO and NgBN but also other elusive noble gas complexes. This invites the theoretical investigation of the conceivable existence of further anionic species XNgY⁻. Experiments could be also performed, for example, in cold matrices to attempt the preparation of these novel noble gas anions.

Acknowledgment. We thank the Italian Ministero dell'Università e della Ricerca (MiUR) for financial support.

References and Notes

- (1) Greenwood, N. N.; Earnshaw, A. In *Chemistry of the Elements*; Butterworth-Heinemann: Oxford, U.K., 2001; p 888.
- (2) Bartlett, N. *Proc. Chem. Soc.* **1962**, 218.
- (3) Lehmann, J. F.; Mercier, H. P. A.; Schrobilgen, G. J. *Coord. Chem. Rev.* **2002**, 233–234, 1.
- (4) Cotton, F. A.; Wilkinson, G. *Advanced Inorganic Chemistry*; Wiley: New York, 1999.
- (5) Gerken, M.; Schrobilgen, G. J. *Coord. Chem. Rev.* **2000**, 197, 335.
- (6) Fields, P. R.; Stein, L.; Zirin, M. H. *J. Am. Chem. Soc.* **1962**, 84, 4164.
- (7) Khriachtchev, L.; Pettersson, M.; Runeberg, N.; Lundell, J.; Räsänen, M. *Nature* **2000**, 406, 874.
- (8) Lignell, A.; Khriachtchev, L.; Lundell, J.; Tanskanen, H.; Räsänen, M. *J. Chem. Phys.* **2006**, 125, 184514 and references therein.
- (9) Wang, M. W. *J. Am. Chem. Soc.* **2000**, 122, 6289.
- (10) Aschi, M.; Grandinetti, F. *Angew. Chem., Int. Ed.* **2000**, 39, 1690.
- (11) Grandinetti, F. *Int. J. Mass Spectrom.* **2004**, 237, 243.
- (12) Krouse, I. H.; Hao, C.; Check, C. E.; Lobring, K. C.; Sunderlin, L. S.; Wenthold, P. G. *J. Am. Chem. Soc.* **2007**, 129, 846.
- (13) Christe, K. O.; Curtis, E. C.; Dixon, D. A.; Mercier, H. P.; Sanders, J. C. P.; Schrobilgen, G. J. *J. Am. Chem. Soc.* **1991**, 113, 3351.
- (14) Christe, K. O.; Dixon, D. A.; Sanders, J. C. P.; Schrobilgen, G. J.; Tsai, S. S.; Wilson, W. W. *Inorg. Chem.* **1995**, 34, 1868.
- (15) Ellern, A.; Seppelt, K. *Angew. Chem., Int. Ed. Engl.* **1995**, 34, 1586.
- (16) Forgeron, M. A. M.; Wasylishen, R. E.; Gerken, M.; Schrobilgen, G. J. *Inorg. Chem.* **2007**, 46, 3585.
- (17) Vallet, V.; Bendazzoli, G. L.; Evangelisti, S. *Chem. Phys.* **2001**, 263, 33.
- (18) Buchachenko, A. A.; Szczyński, M. M.; Klos, J.; Chalasiński, G. *J. Chem. Phys.* **2002**, 117, 2629.
- (19) Viehland, L. A.; Webb, R.; Lee, E. P. F.; Wright, T. G. *J. Chem. Phys.* **2005**, 122, 114302.
- (20) Wright, T. G.; Viehland, L. A. *Chem. Phys. Lett.* **2006**, 420, 24.
- (21) Schröder, D.; Harvey, J. N.; Aschi, M.; Schwarz, H. *J. Chem. Phys.* **1998**, 108, 8446.
- (22) Archibong, E. F.; Hu, C.-H.; Thakkar, A. J. *J. Chem. Phys.* **1998**, 109, 3072.
- (23) (a) Yourshaw, I.; Lenzer, T.; Reiser, G.; Neumark, D. M. *J. Chem. Phys.* **1998**, 109, 5247. (b) Lenzer, T.; Furlanetto, M. R.; Asmis, K. R.; Neumark, D. M. *J. Chem. Phys.* **1998**, 109, 10754. (c) Lenzer, T.; Furlanetto,

- M. R.; Pivonka, N. L.; Neumark, D. M. *J. Chem. Phys.* **1999**, *110*, 6714.
(d) Lenzer, T.; Yourshaw, I.; Furlanetto, M. R.; Pivonka, N. L.; Neumark, D. M. *J. Chem. Phys.* **2002**, *116*, 4170.
- (24) (a) Buchachenko, A. A.; Krems, R. V.; Szczeniński, M. M.; Xiao, Y.-D.; Viehland, L. A.; Chalasiński, G. *J. Chem. Phys.* **2001**, *114*, 9919.
(b) Buchachenko, A. A.; Szczeniński, M. M.; Chalasiński, G. *J. Chem. Phys.* **2001**, *114*, 9929. (c) Buchachenko, A. A.; Tscherbul, T. V.; Klos, J.; Szczeniński, M. M.; Chalasiński, G.; Webb, R.; Viehland, L. A. *J. Chem. Phys.* **2005**, *122*, 194311. (d) Buchachenko, A. A.; Klos, J.; Szczeniński, M. M.; Chalasiński, G.; Gray, B. R.; Wright, T. G.; Wood, E. L.; Viehland, L. A.; Qing, E. *J. Chem. Phys.* **2006**, *125*, 064305.
- (25) Gray, B. R.; Wright, T. G.; Wood, E. L.; Viehland, L. A. *Phys. Chem. Chem. Phys.* **2006**, *8*, 4752.
- (26) Hendricks, J. H.; de Clercq, H. L.; Freidhoff, C. B.; Arnold, S. T.; Eaton, J. G.; Fancher, C.; Lyapustina, S. A.; Snodgrass, J. T.; Bowen, K. H. *J. Chem. Phys.* **2002**, *116*, 7926.
- (27) Adamovic, I.; Gordon, M. S. *J. Phys. Chem. A* **2004**, *108*, 11042.
(28) Botschwina, P.; Oswald, R. *Chem. Phys. Lett.* **2003**, *377*, 156.
(29) (a) Li, T.-H.; Mou, C.-H.; Chen, H.-R.; Hu, W.-P. *J. Am. Chem. Soc.* **2005**, *127*, 9241. (b) Liu, Y.-L.; Chang, Y.-H.; Li, T.-H.; Chen, H.-R.; Hu, W.-P. *Chem. Phys. Lett.* **2007**, *439*, 14.
- (30) Frash, M. V.; Hopkinson, A. C.; Bohme, D. K. *Phys. Chem. Chem. Phys.* **2000**, *2*, 2271.
- (31) Neeser, S.; Voitik, M.; Langhoff, H. *J. Chem. Phys.* **1995**, *102*, 1639.
- (32) Allen, L. C.; Lesk, A. M.; Erdahl, R. M. *J. Am. Chem. Soc.* **1966**, *88*, 615.
- (33) Frenking, G.; Koch, W.; Gauss, J.; Cremer, D. *J. Am. Chem. Soc.* **1988**, *110*, 8007.
- (34) Smith-Gicklhorn, A. M.; Frankowski, M.; Bondybey, V. E. *Mol. Phys.* **2005**, *103*, 11.
- (35) Lin, T.-Y.; Hsu, J.-B.; Hu, W.-P. *Chem. Phys. Lett.* **2005**, *402*, 514.
- (36) Khriachtchev, L.; Lignell, A.; Tanskanen, H.; Lundell, J.; Kiljunen, H.; Räsänen, M. *J. Phys. Chem.* **2006**, *110*, 11876 and references therein.
- (37) Sheng, L.; Cohen, A.; Gerber, R. B. *J. Am. Chem. Soc.* **2006**, *128*, 7156 and references therein.
- (38) McDowell, S. A. C. *J. Chem. Phys.* **2004**, *120*, 9077.
- (39) Baker, J.; Fowler, P. W.; Soncini, A.; Lillington, M. *J. Chem. Phys.* **2005**, *123*, 174309.
- (40) Yockel, S.; Garg, A.; Wilson, A. K. *Chem. Phys. Lett.* **2005**, *411*, 91.
- (41) (a) Ghanty, T. K. *J. Chem. Phys.* **2005**, *123*, 074323. (b) Ghanty, T. K. *J. Chem. Phys.* **2006**, *124*, 124304. (c) Jayasekharan, T.; Ghanty, T. K. *J. Chem. Phys.* **2006**, *125*, 234106.
- (42) Frisch, M. J.; Trucks, G. W.; Schlegel, H. B.; Scuseria, G. E.; Robb, M. A.; Cheeseman, J. R.; Montgomery, J. A., Jr.; Vreven, T.; Kudin, K. N.; Burant, J. C.; Millam, J. M.; Iyengar, S. S.; Tomasi, J.; Barone, V.; Mennucci, B.; Cossi, M.; Scalmani, G.; Rega, N.; Petersson, G. A.; Nakatsuji, H.; Hada, M.; Ehara, M.; Toyota, K.; Fukuda, R.; Hasegawa, J.; Ishida, M.; Nakajima, T.; Honda, Y.; Kitao, O.; Nakai, H.; Klene, M.; Li, X.; Knox, J. E.; Hratchian, H. P.; Cross, J. B.; Adamo, C.; Jaramillo, J.; Gomperts, R.; Stratmann, R. E.; Yazyev, O.; Austin, A. J.; Cammi, R.; Pomelli, C.; Ochterski, J. W.; Ayala, P. Y.; Morokuma, K.; Voth, G. A.; Salvador, P.; Dannenberg, J. J.; Zakrzewski, V. G.; Dapprich, S.; Daniels, A. D.; Strain, M. C.; Farkas, O.; Malick, D. K.; Rabuck, A. D.; Raghavachari, K.; Foresman, J. B.; Ortiz, J. V.; Cui, Q.; Baboul, A. G.; Clifford, S.; Cioslowski, J.; Stefanov, B. B.; Liu, G.; Liashenko, A.; Piskorz, P.; Komaromi, I.; Martin, R. L.; Fox, D. J.; Keith, T.; Al-Laham, M. A.; Peng, C. Y.; Nanayakkara, A.; Challacombe, M.; Gill, P. M. W.; Johnson, B.; Chen, W.; Wong, M. W.; Gonzalez, C.; Pople, J. A. *Gaussian 03*, revision C.02; Gaussian, Inc.: Wallingford, CT, 2004.
- (43) MOLPRO 2000.1 is a package of ab initio programs written by H.-J. Werner and P. J. Knowles, with contributions from R. D. Amos, A. Berning, D. L. Cooper, M. J. O. Deegan, A. J. Dobbyn, F. Eckert, C. Hampel, T. Leininger, R. Lindh, A. W. Lloyd, W. Meyer, M. E. Mura, A. Nicklass, P. Palmieri, K. Peterson, R. Pitzer, P. Pulay, G. Rauhut, M. Schütz, H. Stoll, A. J. Stone, and T. Thorsteinsson.
- (44) (a) Woon, D. E.; Dunning, T. H., Jr. *J. Chem. Phys.* **1993**, *98*, 1358. (b) Kendall, R. A.; Dunning, T. H., Jr.; Harrison, R. J. *J. Chem. Phys.* **1992**, *96*, 6796. (c) Dunning, T. H., Jr. *J. Chem. Phys.* **1989**, *90*, 1007. (d) Peterson, K. A.; Woon, D. E.; Dunning, T. H., Jr. *J. Chem. Phys.* **1994**, *100*, 7410. (e) Wilson, A.; van Mourik, T.; Dunning, T. H., Jr. *J. Mol. Struct. (Theochem)* **1997**, *388*, 339.
- (45) Nicklass, A.; Dolg, M.; Stoll, H.; Preuss, H. *J. Chem. Phys.* **1995**, *102*, 8942.
- (46) Møller, C.; Plesset, M. S. *Phys. Rev.* **1934**, *46*, 618.
- (47) Raghavachari, K.; Trucks, G. W.; Pople, J. A.; Head-Gordon, M. *Chem. Phys. Lett.* **1989**, *157*, 479.
- (48) Hampel, C.; Peterson, K.; Werner, H.-J. *Chem. Phys. Lett.* **1992**, *190*, 1.
- (49) Knowles, P. J.; Hampel, C.; Werner, H.-J. *J. Chem. Phys.* **1993**, *99*, 5219.
- (50) Watts, J. D.; Gauss, J.; Bartlett, R. J. *J. Chem. Phys.* **1993**, *98*, 8718.
- (51) Werner, H.-J.; Knowles, P. J. *J. Chem. Phys.* **1985**, *82*, 5053.
- (52) (a) Glendening, E. D.; Reed, A. E.; Carpenter, J. E.; Weinhold, F. *NBO*, version 3.1. (b) Reed, A. E.; Curtiss, L. A.; Weinhold, F. *Chem. Rev.* **1988**, *88*, 899.
- (53) Breneman, C. M.; Wiberg, K. B. *J. Comput. Chem.* **1990**, *11*, 361.
- (54) (a) Sing, U. C.; Kollman, P. A. *J. Comput. Chem.* **1984**, *5*, 129. (b) Besler, B. H.; Merz, K. M.; Kollman, P. A. *J. Comput. Chem.* **1990**, *11*, 431.
- (55) Bondi, A. J. *Phys. Chem.* **1964**, *68*, 441.
- (56) Bader, R. F. W. *Atoms in Molecules: a Quantum Theory*; Oxford University Press: Oxford, U.K., 1990.
- (57) AIM2000, designed by F. Biegler-König, University of Applied Sciences, Bielefeld, Germany (<http://www.AIM2000.de>).
- (58) Peterson, K. A. *J. Chem. Phys.* **1995**, *102*, 262 and references therein.
- (59) Denis, P. A. *Chem. Phys. Lett.* **2004**, *395*, 12.
- (60) Li, X.; Paldus, J. *Chem. Phys. Lett.* **2006**, *431*, 179.
- (61) Gan, Z.; Grant, D. J.; Harrison, R. J.; Dixon, D. A. *J. Chem. Phys.* **2006**, *125*, 124311.
- (62) Karton, A.; Martin, J. M. L. *J. Chem. Phys.* **2006**, *125*, 144313.
- (63) Lee, T. J.; Taylor, P. R. *Int. J. Quantum Chem. Quantum Chem. Symp.* **1989**, *23*, 199.
- (64) Chen, Y.-L.; Hu, W.-P. *J. Phys. Chem. A* **2004**, *108*, 4449.
- (65) Antonietti, P.; Bronzolino, N.; Grandinetti, F. *J. Phys. Chem. A* **2003**, *107*, 2974.
- (66) Lorenz, M.; Agreiter, J.; Smith, A. M.; Bondybey, V. E. *J. Chem. Phys.* **1996**, *104*, 3143.
- (67) Asmis, K. R.; Taylor, T. R.; Neumark, D. M. *Chem. Phys. Lett.* **1998**, *295*, 75.
- (68) *CRC Handbook of Chemistry and Physics*, 74th ed.; Lide, D. R., Ed.; CRC Press: Boca Raton, FL, 1993.
- (69) Li, T.-H.; Liu, Y.-L.; Lin, R.-J.; Yeh, T.-Y.; Hu, W.-P. *Chem. Phys. Lett.* **2007**, *434*, 38.
- (70) Pyykkö, P. *J. Am. Chem. Soc.* **1995**, *117*, 2067.
- (71) Read, J. P.; Buckingham, A. D. *J. Am. Chem. Soc.* **1997**, *119*, 9010.
- (72) Bader, R. F. W.; Gillespie, R. J.; Martín, F. *Chem. Phys. Lett.* **1998**, *290*, 488.
- (73) Kremer, D.; Kraka, E. *Angew. Chem., Int. Ed. Engl.* **1984**, *23*, 627.
- (74) Bredohl, H.; Dubois, I.; Houbrechts, Y.; Nzohabonayo, P. *J. Phys. B* **1984**, *17*, 95.